Environmental Science & Technology

pubs.acs.org/est

Article

Impact of U.S. Oil and Natural Gas Emission Increases on Surface Ozone Is Most Pronounced in the Central United States

Andrea Pozzer,* Martin G. Schultz, and Detlev Helmig

Cite This: Environ. Sci. Technol. 2020, 54, 12423−12433

Read Online

ACCESS | Metrics & More | Article Recommendations | Supporting Information

ABSTRACT: Observations of volatile organic compounds (VOCs) from a surface sampling network and simulation results from the EMAC (ECHAM5/MESSy for Atmospheric Chemistry) model were analyzed to assess the impact of increased emissions of VOCs and nitrogen oxides from U.S. oil and natural gas (O&NG) sources on air quality. In the first step, the VOC observations were used to optimize the magnitude and distribution of atmospheric ethane and higher-alkane VOC emissions in the model inventory for the base year 2009. Observation-based increases of the emissions of VOCs and NO_x stemming from U.S. oil and natural gas (O&NG) sources during 2009−2014 were then added to the model, and a set of sensitivity runs was conducted for assessing the influence of the increased emissions on summer surface ozone levels. For the year 2014, the added O&NG emissions are predicted to affect surface ozone across a large geographical scale in the United States. These emissions are responsible for an increased number of days when the averaged 8-h ozone values exceed 70 ppb, with the highest sensitivity being in the central and midwestern United States, where most of the O&NG growth has occurred. These findings demonstrate that O&NG emissions significantly affect the air quality across most of the United States, can regionally offset reductions of ozone precursor emissions made in other sectors, and can have a determining influence on a region's ability to meet National Ambient Air Quality Standard (NAAQS) obligations for ozone.

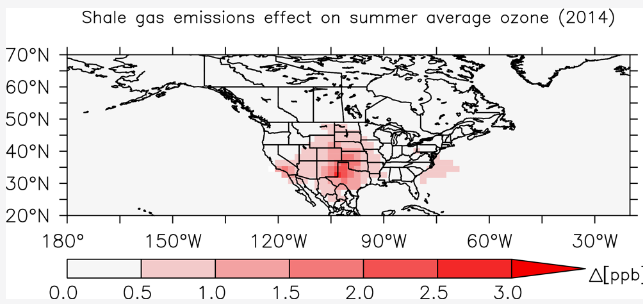

■ INTRODUCTION

During 2010−2015, the combined U.S. oil and natural gas (O&NG) production grew at an unprecedented rate (Supplemental Information (SI) Figure 1), making the United States the largest O&NG producing nation in the world. This growth was stimulated by new technologies, in particular hydraulic fracturing, which enabled the exploration of previously uneconomical shale plays. Atmospheric emissions from heavy drilling equipment, power generation at drill sites, trucking, and controlled and fugitive emissions from well sites, have received attention because of their lasting and reoccurring impacts on air quality, atmospheric chemistry, and climate, from local to global scales.[1−4] Accidental releases, such as during the 2015−2016 Aliso Canyon natural gas blowout, can cause large episodic injections of pollutants into the atmosphere with severe short-term impacts on air quality and human health in the immediate surroundings.[5,6]

Among the pollutants of concern are primary fossil-fuel hydrocarbons, i.e., methane and nonmethane volatile organic compounds (VOCs), as well as nitrogen oxides (NO_x), and black carbon emissions from diesel combustion and flaring.[1,3,7] Measurements within and downwind of O&NG basins have shown at times highly elevated atmospheric levels of VOCs.[8−12] Ground-based monitoring and remote sensing observations have also revealed increased NO_x.[13,14] While elevated VOC levels have been attributed mostly to fugitive emissions from oil and gas drilling, increases in NO_x can be linked to flaring, on-site power generation, and heavy trucking associated to drilling and establishing of the production infrastructure. O&NG emissions have been predicted to contribute to summertime photochemical ozone production based on their chemical reactivity,[15−17] as well as by regional photochemical modeling.[18−22] Two modeling studies have pointed out regional variability of the ozone effects, with potential ozone benefits from the transitioning of coal to O&NG power production.[23,24] O&NG emissions not only foster ozone chemistry during the summer ozone season but also can drive ozone production during snow-covered conditions in winter when ozone precursors are trapped in a shallow surface layer. The high albedo of the snow enhances solar irradiance and increases radical production from carbonyl photolysis, which in turn promotes ozone production.[25−28] As a consequence, the sparsely populated but heavily drilled Uintah Basin reported the highest number of exceedances of

Received: November 19, 2019
Revised: August 6, 2020
Accepted: August 7, 2020
Published: September 9, 2020

the U.S. National Ambient Air Quality Standard (NAAQS) for ozone within the whole United States in 2013,[26,28] thereby challenging the common view of ozone being exclusively a summertime pollution problem. Comparison studies between model outputs and observations of surface ozone levels have pointed to higher top-down flux estimates in O&NG drilling regions than inventory emission estimates,[27,29,30] indicating that modeling based on these inventories has likely tended to underestimate the influence of O&NG emissions on local and regional ozone.

The recent increases seen in the ozone precursor emissions suggest a possible increasing contribution of O&NG emissions to local and regional ozone production, bearing the potential to offset ozone pollution mitigation gains made in other emission sectors.[8] This has brought increasing attention to the role of O&NG emission and their possible compromising role in a region's ability to comply with NAAQS regulations for ozone.[22,31,32] Premature deaths from ozone and PM2.5 resulting from a medium O&NG emission scenario were predicted to increase by 200−460 annually for the Marcellus and Utica shales alone.[22] On the U.S. national scale, premature deaths due to exposure to ozone and $PM_{2.5}$ resulting from O&NG emissions have been estimated to reach 1100−2700 yr^{-1} by 2025.[33]

In a previous preliminary modeling assessment,[10] we applied estimates for increases of C_2−C_5 VOC emission from U.S. O&NG in photochemical modeling. These simulations showed the potential for O&NG emissions to result in up to 0.5 ppb mean summer ozone enhancements, with the largest effects seen over California and the central United States.[10] Here, we expanded on this work, using not only an improved total, spatial, and chemical species distribution of VOCs but also the contribution of NO_x emissions from the growth of U.S. O&NG exploration. This improved representation was then applied to derive an assessment of the regional sensitivity of O&NG emission changes, the contribution of O&NG emissions to regional exceedances of ozone NAAQS, and resulting ozone enhancements across the contiguous United States.

■ METHODS

VOC Observations. The considered VOC observations were from the National Oceanic and Atmospheric Administration (NOAA)/Institute of Arctic and Alpine Research (INSTAAR) Global VOC Monitoring program. This network consists of 44 global background stations within the NOAA Global Greenhouse Gases Reference Network (GGGRN), where pairs of whole air samples are collected weekly and shipped to a central laboratory in Boulder, CO, for C_2−C_7 VOC analyses.[34−36] For this study, we considered the VOC species ethane, propane, *iso-* and *n*-butane, and *iso-* and *n*-pentane, which together constitute the bulk of O&NG nonmethane VOC emissions.[16,17] A list of sites considered in this analysis is provided in SI Table 1.

Ozone Observations. Surface ozone data were from the Tropospheric Ozone Assessment Report (TOAR) data portal.[37] As the focus of this study is on the continental U.S., the data used originated primarily from U.S. sources. For the evaluation of the model runs, only sites with a "rural" characteristic[37] were considered for calculating grid averages. Monthly mean values were calculated at each site, and the data were then aggregated in 2 × 2° grid squares.[38]

Estimation of Growth Rate of U.S. O&NG Emissions. We explored several methods for estimating the rate of increase in U.S. O&NG VOC emissions:

(1) During 2009−2014, U.S. oil and natural gas production increased by 64 and 21%, respectively (SI Figure 1). A simple approach would be to use these growth rates as a surrogate for the emission increase, based on the assumption that emissions scale linearly with the production volume. This assumption is supported by data from a site downwind of the Marcellus Shale, where median ethane measured over four years correlated with the reported shale gas production with an r^2 of 0.59.[9] For the combined oil and natural gas emission increase, one would need to weight these emissions by the relative fraction that oil versus natural gas emissions contributes to total O&NG emissions. An inherent uncertainty is the assumption that the development and production of a new well, mostly due to hydraulic fracturing extraction technologies, are subject to the same fugitive emission loss rate as conventional extraction technologies. This has been questioned by some studies that have pointed out higher emission rates from hydraulic fracturing than from conventional drilling operations.[39−42]

(2) For some O&NG development regions, direct measurements of VOC concentrations provide estimates for O&NG VOC emission rate increases. Increasing atmospheric mole fractions of O&NG-associated VOCs have been reported downwind of the Marcellus Shale[9] and from several sites downwind of O&NG fields in Texas.[8] Data from the GGGRN sites that are near/downwind of O&NG basins show a clear influence from nearby O&NG development and have the highest rates of ethane and propane increase. Rates of increase at Park Falls, Wisconsin, a site downwind of the Bakken Shale, North Dakota, are 7.9 and 13.1% yr^{-1} for ethane and propane, respectively, for June 2009−June 2014. Rates of increase at Southern Great Plains, Oklahoma, a site within the Woodford Shale, are 10.7 and 10.5% yr^{-1}. For Southern Great Plains, similar magnitude growth rates have also been reported for the butane and pentane isomers.[12]

(3) A number of recent publications have developed estimates of the tropospheric ethane increase based on column Fourier transform infrared (FTIR) spectroscopy measurements.[10,43−45] These observations are primarily from remote and/or high elevation sites and are therefore most representative of the ethane growth in the background atmosphere. A review of four publications with a total of ten data sets from seven Northern Hemisphere (NH) sites yields ethane mean/median rates of change of 4.3/4.6% yr^{-1} (SI Table 2). Based on the geographical pattern of increases seen in the shorter-lived propane, the authors argued that this NH troposphere ethane increase largely stems from O&NG emission increases in the United States.

The modeling work presented here was based on the emissions growth that is outlined under point (3) above, which is a lower/conservative emission growth estimate, in comparison to the data and assumptions under (1) and (2). This emission growth was further evaluated by comparison between model and observations as detailed below.

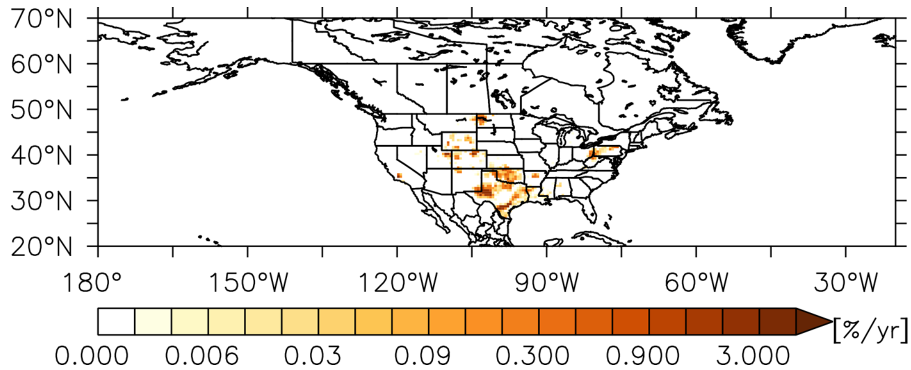

Figure 1. Distribution of O&NG emissions in the continental United States that were added to the model simulations. The color bar shows the emission increase as a fraction of the total (in 2009) in % per year.

Model. We applied the fifth-generation European Centre Hamburg general circulation model (ECHAM5[46]), version 5.3.02, MESSy, version 2.52.0, in the T63L31 resolution, i.e., with a spherical truncation of T63 (corresponding to a quadratic Gaussian grid of approx. 1.9 × 1.9° in latitude and longitude), with 31 vertical hybrid pressure levels up to 10 hPa. Treatment of aerosols has been described previously.[47−49] The model was used in its Chemistry-Transport Model configuration,[50] i.e., without feedback between chemistry and transport. The model was nudged[51] toward the European Centre for Medium-Range Weather Forecast (ECMWF) reanalysis data (ERA-interim,[52]); simulations are covering the period 2009−2014. Further descriptions and evaluations of the ECHAM5 chemistry and model are presented in the literature.[49,53−57] The chemistry mechanism for consideration of the O&NG VOCs was the same as detailed previously,[10] but augmented to include oxidation chemistry of simple C_4−C_5 hydrocarbons (*n*- and *iso*-butane and *n*- and *iso*-pentane), as described in Pozzer et al.[49] Further, a simple mechanism for toluene chemistry was adopted, similar to the approach of Lelieveld et al.[58]

The model simulations adopted emissions from the RCP85 database (Representative Concentration Pathway 8.5),[59] scaled as described in Pozzer et al.[60] To improve the agreement between model results and the observations from VOC monitoring, ethane emissions were further increased by 50% for all emission sources at latitudes north of 20°N. The resulting ethane emissions are as follows: in the NH, 12.1 Tg yr^{-1} of ethane is emitted by anthropogenic sources, 0.2 Tg yr^{-1} by biogenic sources, and 0.9 Tg yr^{-1} by biomass burning, totaling 13.2 Tg yr^{-1} for 2009. With the adjusted emissions, model outputs for the year 2009 agreed with GGGRN observations generally within 10% to the observations (average bias for all the stations worldwide) (SI Figure 2). The adjusted ethane emissions were therefore considered as our default emissions in this work. The propane, butane, and pentane emissions agree with the GGGRN observational data set as shown in Pozzer et al.[49]

Modeled O&NG Emissions. In addition to the standard sector present in the RCP85 database, updated emissions from the O&NG sector were included. The emission map was based on shale O&NG well distribution, available at https://fracfocus.org, which is a different approach than our previous work.[61] This database was considered the most complete, with approximately 2.5 million total well sites registered. This well inventory includes both active and inactive wells. This differentiation will likely only have a minor influence on the results, as the location and density of the wells are deemed to be reasonably proportional to the location of extraction activity, and the relatively large grid scale in the model reduces the uncertainties associated with the relative distribution of retired wells. We assumed that all wells emit the same amounts of VOCs and the same VOC signatures, neglecting differences in well production and leakage rates. Finally, the distributed well map was aggregated in a 0.5 × 0.5° regular map, and emissions were scaled based on the well number density in each grid cell. The resulting emissions map (Figure 1) identifies regions that have experienced recent growth of O&NG development, with regions of large emission increases mostly in the central and northeastern United States.

As enumerated above, we applied an O&NG emission growth rate of ethane of 0.42 Tg/yr^{-2}, consistent with our previous work[10] and equivalent to a ∼17% increase of O&NG emissions over the five-year window (2009−2014). Based on the VOC ratios presented in,[10] we estimated 0.42, 0.30, 0.11, 0.08, 0.05, 0.06, and 0.15 Tg yr^{-2} increases for ethane, propane, *n*-butane, *iso*-butane, *n*-pentane, *iso*-pentane, and toluene emissions every year for five years, respectively. This emission adjustment reflects a global anthropogenic ethane flux increase from 13.2 Tg yr^{-1} in 2009 to 15.3 Tg yr^{-1} in 2014.

Several other recent studies have identified a low bias of O&NG emissions in inventories and proposed inventory emission increases. Our estimates of 13.2 and 15.3 Tg yr^{-1} global ethane emissions for 2009 and 2014, respectively, reflect progressively higher global ethane fluxes similar to other recently updated inventory estimates (i.e., 18.7 Tg yr^{-1} (global, 2014),[45] 12.6 Tg yr^{-1} (global, 2010),[62] and 20 Tg yr^{-1} (global, 2011)).[63]

Although most of the global VOC emission increase identified by Helmig et al.[10] is probably from emissions in the United States, other global regions may have contributed to the flux increase. To reflect and compensate for this uncertainty, VOC emissions $>C_5$ were excluded as they could not unambiguously be identified as emitted by O&NG. Their relative fraction (of total VOCs) can vary over a wide range; on average, they constitute on the order of 10% of the total O&NG VOC emissions.[16,17,64] These longer chain and aromatic VOC generally have higher reactivity and ozone production potential than the lighter nonmethane hydrocarbons (NMHCs).[65]

The methane data were nudged[66] on the surface mimicking the observed values for the simulated period. Although the background methane oxidation is considered in the model, we did not consider increases in regional O&NG methane

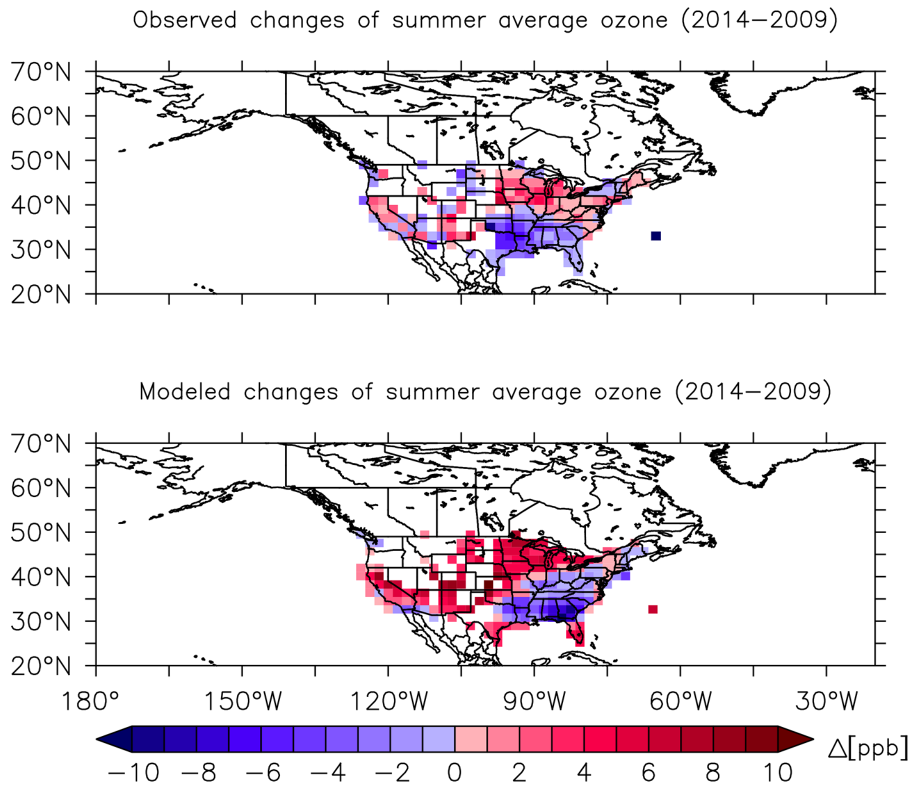

Figure 2. *Model_Run_O&NG_Trend* output for 2014−2009 mean summer ozone changes (top) compared to the ozone changes over the same time interval seen in Tropospheric Ozone Assessment Report (TOAR)[37] data extracted for grid cells with available observations (bottom). The corresponding model output for the entire domain is available in SI Figure 6.

emissions, which can have a further impact on regional ozone production.[67,68] The disregard of emissions of the O&NG longer chain (>C_5), aromatic VOCs, and methane emissions, make it more likely that the results for the estimated O&NG ozone production increase are a lower limit.

In addition to VOCs, O&NG operations also emit nitrogen oxides (NO_x).[13,14] The NO_x emission rates from oil and gas hydraulic fracturing well site development stem from a variety of diverse sources that depend on operator practices and State regulations. The relative ratio of NO_x/VOC emissions from O&NG operations can be quite variable, depending on the abundance and technology of flaring, power generation, and other industry practices,[7,13,69] as well as emissions from the traffic at well sites.[70] Resulting emission rates are likely highly variable, and at this time poorly defined and uncertain. Here, we chose a representation of NO_x emissions in our simulations based on Ahmadov et al.[27] and applied their estimated bottom-up NO_x/VOCs mass emission ratio of 0.023, which we considered the best available estimate for the time represented by the modeling window. We applied this ratio to a total VOC O&NG emission increase estimate of 1.2 Tg yr^{-2}.[10] resulting in a 0.026 Tg yr^{-2} increase of O&NG NO_x emissions, emitted as NO in the model. Potential NO_x emission reductions from the conversion of coal to O&NG power production and potentially associated ozone benefits[23,24] are considered in RCP85.

Model Sensitivity Runs. ECHAM5-MESSy tends to overestimate surface ozone in comparison to observations,[71] similar to what has been noted for other chemistry−climate models.[72,73] Because of the recognition of this potential bias, we intentionally avoided building interpretations on modeled absolute ozone results. Instead, we determined the sensitivity to emission changes from relative differences between model run scenarios. The absolute bias cancels out in these calculations, making results more robust since they are relatively immune to the bias in modeled absolute ozone. In this work, three numerical simulations were performed with the model.

Model_Run_Constant. All emissions were kept constant throughout the years 2009−2014 (i.e., every year has the same emissions as the year 2009). This simulation served as a baseline to determine the effect of meteorology alone on the ozone changes over the investigation period.

Model_Run_RCP85. All emissions were following the RCP85 database as described above, without any new O&NG emissions.

Model_Run_O&NG_Trend. The same as the *Model_Run_RCP85* simulation, with C_2−C_5 NMHC, toluene, and NO_x emissions from shale gas emissions added, increasing from May 2009 to May 2014 as discussed above. (Please note that changes in a reactive and highly variable gas such as ozone over a five-year window may not necessarily imply a "trend." While we avoided the use of the word "trend" in the text, this term was designated as a label for the model runs that used the increasing O&NG emissions.)

NAAQS Exceedances and Ozone Increase Rates. The NAAQS exceedances were calculated as the number of days in a year when the daily maxima of 8-h running mean for ozone exceeded 70 × 10^{-9} mol/mol (ppb), following the U.S. Environmental Protection Agency (EPA) definition (www.epa.gov/outdoor-air-quality-data/air-data-ozone-exceedances). The 2009−2014 rates of change in ozone were calculated following the NOAA trend analysis tool,[74] as described

https://dx.doi.org/10.1021/acs.est.9b06983
Environ. Sci. Technol. 2020, 54, 12423−12433

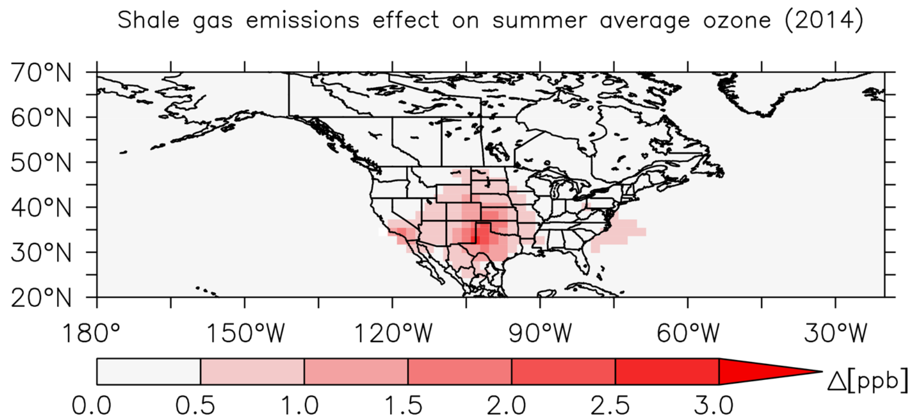

Figure 3. Difference in summer 24 h mean surface ozone between the *Model_Run_O&NG_Trend* versus the *Model_Run_RCP*85 simulation for the year 2014. These results reflect the impact of added O&NG emission on surface ozone.

previously,[10] both for the model and the observational data sets.

RESULTS AND DISCUSSION

Model Evaluation. The ethane model results of the simulation that gave the closest agreement with the data (*Model_Run_O&NG_Trend)* reproduced the observed ethane mixing ratios for most comparisons within 10% (SI Figure 2). Further, the ethane rates of concentration increase that were calculated from the data and the modeled rates of increase were compared for each location for the years 2009−2014 (SI Figure 3). In total, 91% of the results from both methods agree in the sign of the rate of change (increase) and 48% within a factor of two (modeled rate of increase relative to the observed value between 0.5 and 2). It needs to be emphasized that due to the variability in the data, and the relatively short (5 years) time window that was considered, for a significant number of cases, the calculations for the rate of changes in the measurement data had a relatively high uncertainty error (see Supplementary Information to ref 10), which contributes significantly to the deviations in this comparison.

Ozone Changes during 2009−2014. Figure 2 shows the difference between the modeled summer average ozone on the surface for the year 2014 relative to 2009, with the available individual site ozone rate of change observations (SI Figure 4) assembled in each grid to match the model grid cell output. The upper graph shows the observation, and the graph underneath shows the results from the simulations (organized in the same resolution as the model grid size). Model output results are only shown for cells where observations are available to facilitate the comparison. Both analyses show large spatial differences in ozone changes during this time window. There is a good agreement (i.e., within 50%) for the southeastern United States, with ozone decreases of 2−6 ppb during the simulation period. Similarly, there is a good agreement for the central and north-central United States, where observations and the model indicate 1−7 ppb ozone increases. Overall, ozone increases in the model results are larger and geographically wider spread than in the observations. Incorporating the results from the full model domain (SI Figure 5) further emphasizes the prominence of the ozone increase across most of the North American continent, as well as North Pacific and North Atlantic.

The existence and large geographical spread of increasing ozone are rather surprising, as other recent research studies have shown long-term decreasing ozone in the continental United States and the downwind North Atlantic post year 2000.[72,75−77] Further investigation of ozone time series and rate of change analysis outputs from the selected North American ozone monitoring sites (SI Figure 6) demonstrated the cause for this at first seemingly contradictory finding: 2009 and 2010 were relatively low ozone years, followed by 2 years with above-average ozone. These ozone differences are probably linked to meteorological differences in these years that affected ozone production. Over the north-central United States, average temperatures during 2012 were approximately 1.6 K higher than those during 2009.[78] It is therefore likely that these dynamic/meteorological differences and interannual variability in meteorological conditions, in particular the perseverance of high-pressure systems, caused above-average summer temperatures and above-average surface ozone. Previous research has estimated increases of 2−6 ppb of ozone for each K increase in the temperature.[79,80] This sensitivity and these interannual weather differences most likely caused a marked upward/increasing ozone change during the 2009−2014 time period for the north-central United States that defines the long-term ozone trends. These ozone changes are therefore likely largely due to the year-to-year variability and overall relatively warmer weather during the latter part of the chosen five-year time interval and are not a reflection of long-term changes in ozone precursor emissions, including from the O&NG sector.

Effect of O&NG Emissions on Summer Mean Ozone. Using a differential atmospheric modeling approach that considered actual meteorological conditions provided estimates for added ozone production from the growth of O&NG emissions. The sensitivity study included our current best estimate of O&NG emission increases of methane, VOCs, and NO_x over the 2009−2014 growth period. To remove the influence of meteorology, the effect of the O&NG emissions on surface ozone was assessed by subtracting the 2014 model output with the scenario that did not include the O&NG emission increases, i.e., the *Model_Run_RCP*85, from the *Model_Run_O&NG_Trend* simulation. Their difference, shown in Figure 3, is insensitive to meteorological and other emission changes (as they cancel out), and therefore only show the ozone changes due to increasing O&NG emissions. There is high spatial variability in this ozone contribution across the United States. Mean summer ozone increases of ≥1 ppb are observed for more than half of the continental United States,

https://dx.doi.org/10.1021/acs.est.9b06983
Environ. Sci. Technol. 2020, 54, 12423−12433

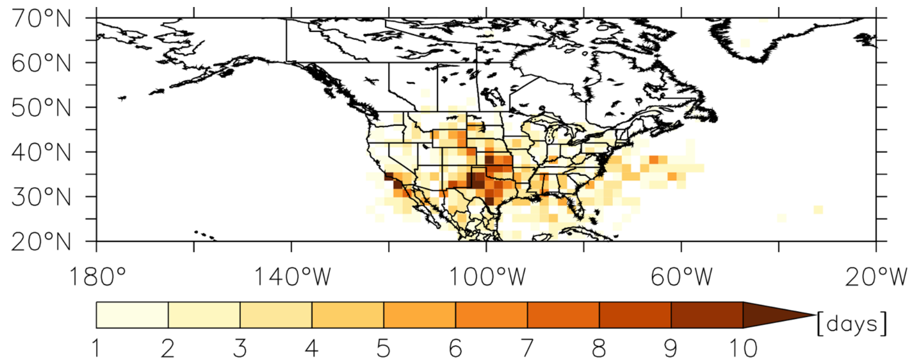

Figure 4. Simulated number of additional days with 8 h summer ozone in 2014 above 70 ppb due to the O&NG 2009−2014 emission increase. Shown are the differences from the *Model_Run_O&NG_Trend* versus the *Model_Run_RCP85* simulations.

with the highest effect seen in the central United States, specifically in Northern Texas, New Mexico, Oklahoma, and Colorado, where ozone increases of up to 3 ppb are modeled. Ozone increases of 1−2 ppb are also modeled for Southern California. Increases of 0.5−1 ppb are seen over the Atlantic downwind of U.S. southeastern states.

These summer ozone increases are ∼20% higher than our previous estimates,[10] which is primarily due to the combined inclusion of O&NG emissions of higher VOCs and NO_x. This relatively small difference illustrates that the contribution of the O&NG NO_x emission is relatively small (<20%) compared to the O&NG VOC emissions. Furthermore, the increases in ozone are now more pronounced in the central United States, reflecting the updated distribution of emissions increase. Notable ozone increases are also seen over selected areas in southern California. This finding is a bit surprising, as emission increases in California are relatively small (Figure 1). This high sensitivity is primarily due to high NO_x conditions in this region, which causes relatively modest increases in VOC emissions to have a relatively large influence on ozone production.

Two other previous studies have provided estimates of the recent O&NG increase in U.S. surface ozone. Kort et al.[21] show a sensitivity study that considered fugitive alkane (C_2 and higher) emissions from the Bakken Shale only. For one particular day in August 2014, they calculated ozone increases at and downwind of the primary emission locations in North and South Dakota, and eastern Montana, reaching 2 ppb. Tzompa et al.,[81] applying updated O&NG emission fields to the GEOS-Chem CTM, predicted daytime summer ozone increases of up to 4 ppb, with the strongest effect seen over the central United States, which is reasonably consistent with our findings.

Effect of O&NG Emissions on Regulatory Summer 8-h Mean Ozone Metrics. The U.S. ozone compliance with NAAQS is defined by the "Design Value," which is calculated as the mean of three consecutive years of the fourth highest annual value for the daily maximum average 8-h ozone value (MDA8).[82] As we simulated a limited amount of years, we decided instead to estimate the number of days for individual years when the MDA8 exceeded 70 ppb, which is a metric also largely used by the EPA.[83] For instance, for the year 2014, the model predicts that the ozone production from the added O&NG emissions caused 0−10 additional days when the MDA8 exceeded 70 ppb over regions in the contiguous United States, with 90% of the United States affected by at least one additional exceedance day (Figure 4).

Additional exceedance days from the growth of the O&NG emissions are observed in most of the continental United States, with the exception of Alaska. Approximately 90% of the contiguous United States experienced at last one additional day with 8 h surface ozone >70 ppb. These results for ozone standard exceedance days display a higher regional sensitivity than the previously reported results for average ozone increases.[33,81] It must be stressed that these results are rather sensitive to the particular regional meteorological conditions in the chosen model year. The chosen year 2014 was, for instance, a relatively low ozone year in the central United States ([32],[84] SI Figure 6), which would tend to produce a relatively lower number of ozone exceedances for that region and particular year. It must, however, also be stressed that the model in general tends to overpredict the absolute ozone concentrations on the surface (see the discussion above and ref[71]), which has the effect of overestimating the absolute number of MDA8 exceedances compared to the EPA observations. This is particularly pronounced in the few comparison locations in the central-southern United States, whereas a relatively better agreement was found for the western regions (see also section "Policy Implications" for a discussion on uncertainties). For estimating this bias, we performed an alternative calculation, where the year 2014-modeled ozone from the added O&NG emission was subtracted from the observational data. This resulted in a sensitivity of -1−12 exceedance days (compared to 0−28 days) and an overall lower fraction of the stations with an increase of at least one exceedance day, i.e., ∼5 vs 67%. There is a notable overlap of regions with a high number of added high ozone days and areas that are in nonattainment with the ozone NAAQS (SI Figure 8). The impact is most pronounced on a wider geographical scale in the central United States. Hence, although meteorology is the main driver of ozone increase in the 2009−2014 period, the O&NG emissions have the effect of further promoting possible ozone NAAQS exceedances in this region.

A preliminary assessment of the health effects projected on the order of 320 (298−344 at a confidence level of 95%) additional premature deaths from the added ozone per year (SI Text 1; please note that this mortality estimate does not include possible reductions in mortality from the decreased emissions that result from the transition of coal- to natural-gas-powered electricity-generating plants). According to the assessment in Fann et al.,[33] health effects from fine particulate matter produced by O&NG emission are of a similar magnitude; therefore, the total mortality rate from O&NG-

https://dx.doi.org/10.1021/acs.est.9b06983
Environ. Sci. Technol. 2020, 54, 12423−12433

produced ozone and PM2.5 is possibly on the order of two times the ozone estimate.

Policy Implications. A notable finding is that ozone increases are predicted across large geographical scales across most of the United States. This also includes numerous regions and States that do not have seen significant increases of O&NG industries within their own borders. Results reflecting a smaller, i.e., regional geographical scale bear a higher uncertainty due to the relatively coarse ($1.8 \times 1.8°$, i.e., ~200 km × ~200 km) model resolution. Additional sources of uncertainties include the neglect of the contribution of ozone production from regional methane emissions, the omission of higher O&NG VOC species, and a conservative emission growth estimate (see above) for primary O&NG development regions. Diurnal ozone production occurs on time scales that are shorter than the transport scales and mixing regimes within the model grids; consequently, ozone production and exceedances can be higher or lower at selected locations within a grid. It is therefore likely that our O&NG ozone production estimates are over predictions in some regions and under predictions in other regions. It is well possible that a higher number of added exceedances occur on smaller geographical scales and in closer proximity to emission sources. Further, our investigations exclusively focused on summer ozone, as winter ozone chemistry under conditions of surface snow cover, low boundary layer heights, and the particular chemical conditions, resulting in high ozone production rates, is currently not well presented in the model. Elevated ozone and NAAQS exceedances during winter have been observed in the Uintah Basin, Utah, and Upper Green River Valley, Wyoming. These conditions and events were not included in this evaluation. Consequently, our estimates of the increased O&NG emissions on ozone and air quality regulation compliance, excluding these winter ozone episodes must be taken with caution, and are likely a low estimate of the year-round impacts of emissions on ozone air quality in these O&NG basins.

This research had the objective to investigate the regional to large-scale effects of increased O&NG emission by a differential modeling approach. An inherent weakness stems from the lack of regional/basin specific emission speciation and emission rates. Regulations on O&NG operation and emission controls vary by states, and the rate of controlled and fugitive emissions varies widely depending on many conditions, including the chemical composition of the petroleum reservoir, operator equipment, practices, and on the stage of well development.[85] Our modeling attributed emissions equally among all reported wells, neglecting any of these dependencies, which contribute to the uncertainty in the regional sensitivity of our findings. There is also the potential of a reduction in ozone precursor emissions in the proximity and downwind of electrical power plants that were converted from coal to gas as a consequence of the lower cost and readily available gas for power generation.[24] As stated by the authors of this publication,[24] the combined effects will likely vary regionally depending on the location and overlap of O&NG basins and processing facility in relation to the location of power generation plants, and need to be evaluated on a regional case-by-case basis.

Our studies demonstrate that the assessment of air quality impacts of the rapidly growing U.S. O&NG industry would largely benefit from a more accurate characterization of the chemical emissions and their regional variations. Further, policy implementation for emission reductions from O&NG industries bear the potential to reduce ozone production and improve air quality within, and in adjacent and downwind areas, including neighboring states. These reductions would be particularly advantageous for several ozone non-attainment areas to reach compliance with the ozone NAAQS[18,21,86−88] and would furthermore be beneficial for downwind regions across wide areas of the United States.

■ ASSOCIATED CONTENT

Supporting Information

The Supporting Information is available free of charge at https://pubs.acs.org/doi/10.1021/acs.est.9b06983.

List of sites, sorted by latitude, within the GGGRN (Table 1); growth rate of atmospheric ethane (Table 2); oil and natural gas production trends in the United States (Figure 1); comparison of Global Greenhouse Gas Reference Network observations with the *Model_Run_O&NG_Trend* simulation results (Figure 2); comparison of GGGRN ethane trends (Figure 3); year 2009−2014 surface ozone trends at TOAR sites (Figure 4); 2009−2014 mean summer ozone changes (Figure 5); ozone output from the model for a midwestern U.S. location (Figure 6); enlargements of results shown in Figure 3 (Figure 7); U.S. map showing counties that as of September 2018 were in nonattainment of the 2015 ozone NAAQS (Figure 8); and mortality estimate (Text 1) (PDF)

■ AUTHOR INFORMATION

Corresponding Author

Andrea Pozzer − *Max Planck Institute for Chemistry, 55128 Mainz, Germany*; Email: andrea.pozzer@mpic.de

Authors

Martin G. Schultz − *Jülich Supercomputing Centre, Forschungszentrum Jülich GmbH, 52425 Jülich, Germany*

Detlev Helmig − *Institute of Arctic and Alpine Research, University of Colorado, Boulder, Colorado 80305, United States*

Complete contact information is available at: https://pubs.acs.org/10.1021/acs.est.9b06983

Notes

The authors declare no competing financial interest.

■ ACKNOWLEDGMENTS

The chemical modeling work by MGS was funded through the PoF III program of the Helmholtz Association, Germany. The VOC analyses at INSTAAR were conducted in samples collected for NOAA's Global Greenhouse Gas Reference Network, which is operated by the NOAA Global Monitoring Laboratory. NOAA also provided support for the VOC analysis. We thank all personnel who are involved in the management and execution of this program. We also thank all colleagues and agencies who generate and publicly share meteorological and chemical data that were used as inputs in the atmospheric modeling. The authors acknowledge the use of the Ferret program for analyses and graphics in this paper. Ferret is a product of NOAA's Pacific Marine Environmental Laboratory (information is available at http://ferret.pmel.noaa.gov/Ferret/).

REFERENCES

(1) Field, R. A.; Soltis, J.; Murphy, S. Air quality concerns of unconventional oil and natural gas production. *Environ. Sci. Process. Impacts* **2014**, *16*, 954−969.

(2) Moore, C. W.; Zielinska, B.; Petron, G.; Jackson, R. B. Air Impacts of Increased Natural Gas Acquisition, Processing, and Use: A Critical Review. *Environ. Sci. Technol.* **2014**, *48*, 8349−8359.

(3) Adgate, J. L.; Goldstein, B. D.; McKenzie, L. M. Potential Public Health Hazards, Exposures and Health Effects from Unconventional Natural Gas Development. *Environ. Sci. Technol.* **2014**, *48*, 8307−8320.

(4) Allen, D. T. Emissions from oil and gas operations in the United States and their air quality implications. *J. Air Waste Manage. Assoc.* **2016**, *66*, 549−575.

(5) Conley, S.; Franco, G.; Faloona, I.; Blake, D. R.; Peischl, J.; Ryerson, T. B. Methane emissions from the 2015 Aliso Canyon blowout in Los Angeles, CA. *Science* **2016**, *351*, 1317−1320.

(6) Jacobson, M. Z. Short-term impacts of the Aliso Canyon natural gas blowout on weather, climate, air quality, and health in California and Los Angeles. *Environ. Sci. Technol.* **2019**, *53*, 6081−6093.

(7) Schade, G. W.; Roest, G. Source apportionment of non-methane hydrocarbons, NOx and H_2S data from a central monitoring station in the Eagle Ford shale, Texas. *Elementa Sci. Anthropocene* **2018**, *6*, 35.

(8) Schade, G. W.; Roest, G. S. Is the shale boom reversing progress in curbing ozone pollution? In. *EOS* **2015**, *96*, 1−8.

(9) Vinciguerra, T.; Yao, S.; Dadzie, J.; Chittams, A.; Deskins, T.; Ehrman, S.; Dickerson, R. R. Regional air quality impacts of hydraulic fracturing and shale natural gas activity: Evidence from ambient VOC observations. *Atmos. Environ.* **2015**, *110*, 144−150.

(10) Helmig, D.; Rossabi, S.; Hueber, J.; Tans, P.; Montzka, S.; Masarie, K.; Thoning, K.; Plass-Duelmer, C.; Claude, A.; Carpenter, L.; Lewis, A. C.; Punjabi, S.; Reimann, S.; Vollmer, M.; Steinbrecher, R.; Hannigan, J.; Emmons, L.; Mahieu, E.; Franco, B.; Smale, D.; Pozzer, A. Reversal of global atmospheric ethane and propane trends largely due to US Oil and natural gas production. *Nat. Geosci.* **2016**, *9*, 490−495.

(11) Schade, G. W.; Roest, G. Analysis of non-methane hydrocarbon data from a monitoring station affected by oil and gas development in the Eagle Ford shale, Texas. *Elementa Sci. Anthropocene* **2016**, *4*, 000096.

(12) Rossabi, S.; Helmig, D. Changes in atmospheric butanes and pentanes and their isomeric ratios in the Continental United States. *J. Geophys. Res.: Atmos.* **2018**, *123*, 3772−3790.

(13) Duncan, B. N.; Lamsal, L. N.; Thompson, A. M.; Yoshida, Y.; Lu, Z.; Streets, D. G.; Hurwitz, M. M.; Pickering, K. E. A space-based, high-resolution view of notable changes in urban NOx pollution around the world (2005-2014). *J. Geophys. Res.: Atmos.* **2016**, *121*, 976−996.

(14) Majid, A.; Martin, M. V.; Lamsal, L. N.; Duncan, B. N. A decade of changes in nitrogen oxides over regions of oil and natural gas activity in the United States. *Elementa Sci. Anthropocene* **2017**, *5*, 76.

(15) Swarthout, R. F.; Russo, R. S.; Zhou, Y.; Miller, B. M.; Mitchell, B.; Horsman, E.; Lipsky, E.; McCabe, D. C.; Baum, E.; Sive, B. C. Impact of Marcellus Shale Natural Gas Development in Southwest Pennsylvania on Volatile Organic Compound Emissions and Regional Air Quality. *Environ. Sci. Technol.* **2015**, *49*, 3175−3184.

(16) Swarthout, R. F.; Russo, R. S.; Zhou, Y.; Hart, A. H.; Sive, B. C. Volatile organic compound distributions during the NACHTT campaign at the Boulder Atmospheric Observatory: Influence of urban and natural gas sources. *J. Geophys. Res.: Atmos.* **2013**, *118*, 10614−10637.

(17) Gilman, J. B.; Lerner, B. M.; Kuster, W. C.; de Gouw, J. A. Source signature of volatile organic compounds from oil and natural gas operations in northeastern Colorado. *Environ. Sci. Technol.* **2013**, *47*, 1297−1305.

(18) Olaguer, E. P. The potential near-source ozone impacts of upstream oil and gas industry emissions. *J. Air Waste Manage. Assoc.* **2012**, *62*, 966−977.

(19) Kemball-Cook, S.; Bar-Ilan, A.; Grant, J.; Parker, L.; Jung, J. G.; Santamaria, W.; Mathews, J.; Yarwood, G. Ozone impacts of natural gas development in the Haynesville Shale. *Environ. Sci. Technol.* **2010**, *44*, 9357−9363.

(20) Ahmadi, M.; John, K. Statistical evaluation of the impact of shale gas activities on ozone pollution in North Texas. *Sci. Total Environ.* **2015**, *536*, 457−467.

(21) Kort, E. A.; Smith, M. L.; Murray, L. T.; Gvakharia, A.; Brandt, A. R.; Peischl, J.; Ryerson, T. B.; Sweeney, C.; Travis, K. Fugitive emissions from the Bakken shale illustrate role of shale production in global ethane shift. *Geophys. Res. Lett.* **2016**, *43*, 4617−4623.

(22) Roohani, Y. H.; Roy, A. A.; Heo, J.; Robinson, A. L.; Adams, P. J. Impact of natural gas development in the Marcellus and Utica shales on regional ozone and fine particulate matter levels. *Atmospheric Environment* **2017**, *155*, 11−20.

(23) Pacsi, A. P.; Alhajeri, N. S.; Zavala-Araiza, D.; Webster, M. D.; Allen, D. T. Regional Air Quality Impacts of Increased Natural Gas Production and Use in Texas. *Environ. Sci. Technol.* **2013**, *47*, 3521−3527.

(24) Pacsi, A. P.; Kimura, Y.; McGaughey, G.; McDonald-Buller, E. C.; Allen, D. T. Regional Ozone Impacts of Increased Natural Gas Use in the Texas Power Sector and Development in the Eagle Ford Shale. *Environ. Sci. Technol.* **2015**, *49*, 3966−3973.

(25) Schnell, R. C.; Oltmans, S. J.; Neely, R. R.; Endres, M. S.; Molenar, J. V.; White, A. B. Rapid photochemical production of ozone at high concentrations in a rural site during winter. *Nat. Geosci.* **2009**, *2*, 120−122.

(26) Oltmans, S.; Schnell, R. C.; Johnson, B.; Petron, G.; Mefford, T.; Neely, R. N. I. Anatomy of wintertime ozone associated with oil and natural gas extraction activity in Wyoming and Utah. *Elementa Sci. Anthropocene* **2014**, *2*, 000024.

(27) Ahmadov, R.; McKeen, S.; Trainer, M.; Banta, R.; Brewer, A.; Brown, S.; Edwards, P. M.; de Gouw, J. A.; Frost, G. J.; Gilman, J.; Helmig, D.; Johnson, B.; Karion, A.; Koss, A.; Langford, A.; Lerner, B.; Olson, J.; Oltmans, S.; Peischl, J.; Petron, G.; Pichugina, Y.; Roberts, J. M.; Ryerson, T.; Schnell, R.; Senff, C.; Sweeney, C.; Thompson, C.; Veres, P. R.; Warneke, C.; Wild, R.; Williams, E. J.; Yuan, B.; Zamora, R. Understanding high wintertime ozone pollution events in an oil- and natural gas-producing region of the western US. *Atmos. Chem. Phys.* **2015**, *15*, 411−429.

(28) Edwards, P. M.; Brown, S. S.; Roberts, J. M.; Ahmadov, R.; Banta, R. M.; deGouw, J. A.; Dube, W. P.; Field, R. A.; Flynn, J. H.; Gilman, J. B.; Graus, M.; Helmig, D.; Koss, A.; Langford, A. O.; Lefer, B. L.; Lerner, B. M.; Li, R.; Li, S.-M.; McKeen, S. A.; Murphy, S. M.; Parrish, D. D.; Senff, C. J.; Soltis, J.; Stutz, J.; Sweeney, C.; Thompson, C. R.; Trainer, M. K.; Tsai, C.; Veres, P. R.; Washenfelder, R. A.; Warneke, C.; Wild, R. J.; Young, C. J.; Yuan, B.; Zamora, R. High winter ozone pollution from carbonyl photolysis in an oil and gas basin. *Nature* **2014**, *514*, 351−354.

(29) Matichuk, R.; Tonnesen, G.; Luecken, D.; Gilliam, R.; Napelenok, S. L.; Baker, K. R.; Schwede, D.; Murphy, B.; Helmig, D.; Lyman, S. N.; Roselle, S. Evaluation of the Community Multiscale Air Quality Model for Simulating Winter Ozone Formation in the Uinta Basin. *J. Geophys. Res.: Atmos.* **2017**, *122*, 13545−13572.

(30) Pétron, G.; Frost, G.; Miller, B. R.; Hirsch, A. I.; Montzka, S. A.; Karion, A.; Trainer, M.; Sweeney, C.; Andrews, A. E.; Miller, L.; Kofler, J.; Bar-Ilan, A.; Dlugokencky, E. J.; Patrick, L.; Moore, C. T.; Ryerson, T. B.; Siso, C.; Kolodzey, W.; Lang, P. M.; Conway, T.; Novelli, P.; Masarie, K.; Hall, B.; Guenther, D.; Kitzis, D.; Miller, J.; Welsh, D.; Wolfe, D.; Neff, W.; Tans, P. Hydrocarbon emissions characterization in the Colorado Front Range: A pilot study. *J. Geophys. Res.: Atmos.* **2012**, *117*, 1−19.

(31) Cheadle, L. C.; Oltmans, S. J.; Pétron, G.; Schnell, R. C.; Mattson, E. J.; Herndon, S. C.; Thompson, A. M.; Blake, D. R.; McClure-Begley, A. Surface ozone in the Colorado northern Front Range and the influence of oil and gas development during FRAPPE/DISCOVER-AQ in summer 2014. *Elementa Sci. Anthropocene* **2017**, No. 61.

(32) Evans, J. M.; Helmig, D. Investigation of the influence of transport from oil and natural gas regions on elevated ozone levels in the northern Colorado front range. *J. Air Waste Manage. Assoc.* **2017**, *67*, 196−211.
(33) Fann, N.; Baker, K. R.; Chan, E. A. W.; Eyth, A.; Macpherson, A.; Miller, E.; Snyder, J. Assessing human health PM2.5 and ozone impacts from US oil and natural gas sector emissions in 2025. *Environ. Sci. Technol.* **2018**, *52*, 8095−8103.
(34) Pollmann, J.; Helmig, D.; Hueber, J.; Plass-Dülmer, C.; Tans, P. Sampling, storage, and analysis of C2-C7 non-methane hydrocarbons from the US National Oceanic and Atmospheric Administration Cooperative Air Sampling Network glass flasks. *J. Chromatogr. A* **2008**, *1188*, 75−87.
(35) Helmig, D.; Bottenheim, J.; Galbally, I. E.; Lewis, A.; Milton, M. J. T.; Penkett, S.; Plass-Duelmer, C.; Reimann, S.; Tans, P.; Theil, S. Volatile organic compounds in the global atmosphere. *EOS Trans., Am. Geophys. Union* **2009**, *90*, 513−520.
(36) Schultz, M. G.; Akimoto, H.; Bottenheim, J.; Buchmann, B.; Galbally, I. E.; Gilge, S.; Helmig, D.; Koide, H.; Lewis, A. C.; Novelli, P. C.; Plass-Duelmer, C.; Ryerson, T. B.; Steinbacher, M.; Steinbrecher, R.; Tarasova, O.; Torseth, K.; Thouret, V.; Zellweger, C. The Global Atmosphere Watch reactive gases measurement network. *Elementa Sci. Anthropocene* **2015**, *3*, 000067.
(37) Schultz, M. G.; Schroder, S.; Lyapina, O.; Cooper, O. R.; Galbally, I.; Petropavlovskikh, I.; von Schneidemesser, E.; Tanimoto, H.; Elshorbany, Y.; Naja, M.; Seguel, R. J.; Dauert, U.; Eckhardt, P.; Feigenspan, S.; Fiebig, M.; Hjellbrekke, A. G.; Hong, Y. D.; Kjeld, P. C.; Koide, H.; Lear, G.; Tarasick, D.; Ueno, M.; Wallasch, M.; Baumgardner, D.; Chuang, M. T.; Gillett, R.; Lee, M.; Molloy, S.; Moolla, R.; Wang, T.; Sharps, K.; Adame, J. A.; Ancellet, G.; Apadula, F.; Artaxo, P.; Barlasina, M. E.; Bogucka, M.; Bonasoni, P.; Chang, L.; Colomb, A.; Cuevas-Agullo, E.; Cupeiro, M.; Degorska, A.; Ding, A. J.; FrHlich, M.; Frolova, M.; Gadhavi, H.; Gheusi, F.; Gilge, S.; Gonzalez, M. Y.; Gros, V.; Hamad, S. H.; Helmig, D.; Henriques, D.; Hermansen, O.; Holla, R.; Hueber, J.; Im, U.; Jaffe, D. A.; Komala, N.; Kubistin, D.; Lam, K. S.; Laurila, T.; Lee, H.; Levy, I.; Mazzoleni, C.; Mazzoleni, L. R.; McClure-Begley, A.; Mohamad, M.; Murovec, M.; Navarro-Comas, M.; Nicodim, F.; Parrish, D.; Read, K. A.; Reid, N.; Ries, N. R. L.; Saxena, P.; Schwab, J. J.; Scorgie, Y.; Senik, I.; Simmonds, P.; Sinha, V.; Skorokhod, A. I.; Spain, G.; Spangl, W.; Spoor, R.; Springston, S. R.; Steer, K.; Steinbacher, M.; Suharguniyawan, E.; Torre, P.; Trickl, T.; Lin, W. L.; Weller, R.; Xu, X. B.; Xue, L. K.; Ma, Z. Q. Tropospheric Ozone Assessment Report: Database and metrics data of global surface ozone observations. *Elementa Sci. Anthropocene* **2017**, *5*, No. 58.
(38) Schultz, M. G.; Stadtler, S.; Schroder, S.; Taraborrelli, D.; Franco, B.; Krefting, J.; Henrot, A.; Ferrachat, S.; Lohmann, U.; Neubauer, D.; Siegenthaler-Le Drian, C.; Wahl, S.; Kokkola, H.; Kuhn, T.; Rast, S.; Schmidt, H.; Stier, P.; Kinnison, D.; Tyndall, G. S.; Orlando, J. J.; Wespes, C. The chemistry-climate model ECHAM6.3-HAM2.3-MOZ1.0. *Geosci. Model Dev.* **2018**, *11*, 1695−1723.
(39) Caulton, D. R.; Shepson, P. B.; Santoro, R. L.; Sparks, J. P.; Howarth, R. W.; Ingraffea, A. R.; Cambaliza, M. O. L.; Sweeney, C.; Karion, A.; Davis, K. J.; Stirm, B. H.; Montzka, S. A.; Miller, B. R. Toward a better understanding and quantification of methane emissions from shale gas development. *Proc. Natl. Acad. Sci. U.S.A.* **2014**, *111*, 6237−6242.
(40) Howarth, R. W. A bridge to nowhere: Methane emissions and the greenhouse gas footprint of natural gas. *Energy Sci. Eng.* **2014**, *2*, 47−60.
(41) Karion, A.; Sweeney, C.; Petron, G.; Frost, G.; Hardesty, M.; Kofler, J.; Miller, B. R.; Newberger, T.; Wolter, S.; Banta, R.; Brewer, A.; Dlugkencky, E. J.; Lang, P.; Montzka, S. A.; Schnell, R. C.; Tans, P.; Trainer, M.; Zomora, R.; Conley, S. Methane emissions estimate from airborne measurements over a western United States natural gas field. *Geophys. Res. Lett.* **2013**, *40*, 4393−4397.
(42) Howarth, R. W. Ideas and perspectives: Is shale gas a major driver of recent increase in global atmospheric methane? *Biogeosciences* **2019**, *16*, 3033−3046.
(43) Hausmann, P.; Sussmann, R.; Smale, D. Contribution of oil and natural gas production to renewed increase of atmospheric methane (2007−2014): Top-down estimate from ethane and methane column observations. *Atmos. Chem. Phys.* **2016**, *16*, 3227−3244.
(44) Franco, B.; Bader, W.; Toon, G. C.; Bray, C.; Perrin, A.; Fischer, E. V.; Sudo, K.; Boone, C. D.; Bovy, B.; Lejeune, B.; Servais, C.; Mahieu, E. Retrieval of ethane from ground-based FTIR solar spectra using improved spectroscopy: Recent burden increase above Jungfraujoch. *J. Quant. Spectrosc. Radiat. Transfer* **2015**, *160*, 36−49.
(45) Franco, B.; Mahieu, E.; Emmons, L. K.; Tzompa-Sosa, Z. A.; Fisher, E. V.; Sudo, K.; Bovy, B.; Conway, S.; Griffin, D.; Hannigan, J.; Strong, K.; Walker, K. A. Evaluating ethane and methane emissions associated with the development of oil and natural gas extraction in North America. *Environ. Res. Lett.* **2016**, *11*, No. 044010.
(46) Roeckner, E.; Brokopf, R.; Esch, M.; Giorgetta, M.; Hagemann, S.; Kornblueh, L.; Manzini, E.; Schlese, U.; Schulzweida, U. Sensitivity of Simulated Climate to Horizontal and Vertical Resolution in the ECHAM5 Atmosphere Model. *J. Clim.* **2006**, *19*, 3771−3791.
(47) de Meij, A.; Pozzer, A.; Pringle, K. J.; Tost, H.; Lelieveld, J. EMAC model evaluation and analysis of atmospheric aerosol properties and distribution with a focus on the Mediterranean region. *Atmos. Res.* **2012**, *114*, 38−69.
(48) Pringle, K. J.; Tost, H.; Pozzer, A.; Poschl, U.; Lelieveld, J. Global distribution of the effective aerosol hygroscopicity parameter for CCN activation. *Atmos. Chem. Phys.* **2010**, *10*, 5241−5255.
(49) Pozzer, A.; de Meij, A.; Pringle, K. J.; Tost, H.; Doering, U. M.; van Aardenne, J.; Lelieveld, J. Distributions and regional budgets of aerosols and their precursors simulated with the EMAC chemistry-climate model. *Atmos. Chem. Phys.* **2012**, *12*, 961−987.
(50) Deckert, R.; Jöckel, P.; Grewe, V.; Gottschaldt, K. D.; Hoor, P. A quasi chemistry-transport model mode for EMAC. *Geosci. Model Dev.* **2011**, *4*, 195−206.
(51) Jeuken, A. B. M.; Siegmund, P. C.; Heijboer, L. C.; Feichter, J.; Bengtsson, L. On the potential of assimilating meteorological analyses in a global climate model for the purpose of model validation. *J. Geophys. Res.: Atmos.* **1996**, *101*, 16939−16950.
(52) Dee, D. P.; Uppala, S. M.; Simmons, A. J.; Berrisford, P.; Poli, P.; Kobayashi, S.; Andrae, U.; Balmaseda, M. A.; Balsamo, G.; Bauer, P.; Bechtold, P.; Beljaars, A. C. M.; van de Berg, L.; Bidlot, J.; Bormann, N.; Delsol, C.; Dragani, R.; Fuentes, M.; Geer, A. J.; Haimberger, L.; Healy, S. B.; Hersbach, H.; Holm, E. V.; Isaksen, L.; Kallberg, P.; Kohler, M.; Matricardi, M.; McNally, A. P.; Monge-Sanz, B. M.; Morcrette, J.-J.; Park, B.-K.; Peubey, C.; de Rosnay, P.; Tavolato, C.; Thepaut, J.-N.; Vitart, F. The ERA-Interim reanalysis: configuration and performance of the data assimilation system. *Q. J. R. Meteorol. Soc.* **2011**, *137* (656), 553−597.
(53) Pöschl, U.; von Kuhlmann, R.; Poisson, N.; Crutzen, P. J. Development and intercomparison of condensed isoprene oxidation mechanisms for global atmospheric modeling. *J. Atmos. Chem.* **2000**, *37*, 29−52.
(54) Jöckel, P.; Tost, H.; Pozzer, A.; Bruhl, C.; Buchholz, J.; Ganzeveld, L.; Hoor, P.; Kerkweg, A.; Lawrence, M. G.; Sander, R.; Steil, B.; Stiller, G.; Tanarhte, M.; Taraborrelli, D.; Van Aardenne, J.; Lelieveld, J. The atmospheric chemistry general circulation model ECHAM5/MESSy1: consistent simulation of ozone from the surface to the mesosphere. *Atmos. Chem. Phys.* **2006**, *6*, 5067−5104.
(55) Pozzer, A.; de Meij, A.; Yoon, J.; Tost, H.; Georgoulias, A. K.; Astitha, M. AOD trends during 2001−2010 from observations and model simulations. *Atmos. Chem. Phys.* **2015**, *15*, 5521−5535.
(56) Saunders, S. M.; Jenkin, M. E.; Derwent, R. G.; Pilling, M. J. Protocol for the development of the Master Chemical Mechanism, MCM v3 (Part A): tropospheric degradation of non-aromatic volatile organic compounds. *Atmos. Chem. Phys.* **2003**, *3*, 161−180.
(57) Sander, R.; Jockel, P.; Kirner, O.; Kunert, A. T.; Landgraf, J.; Pozzer, A. The photolysis module JVAL-14, compatible with the MESSy standard, and the JVal PreProcessor (JVPP). *Geosci. Model Dev.* **2014**, *7*, 2653−2662.

(58) Lelieveld, J.; Gromov, S.; Pozzer, A.; Taraborrelli, D. Global tropospheric hydroxyl distribution, budget and reactivity. *Atmos. Chem. Phys.* **2016**, *16*, 12477−12493.
(59) van Vuuren, D. P.; Edmonds, J.; Kainuma, M.; Riahi, K.; Thomson, A.; Hibbard, K.; Hurtt, G. C.; Kram, T.; Krey, V.; Lamarque, J.-F.; Masui, T.; Meinshausen, M.; Nakicenovic, N.; Smith, S. J.; Rose, S. K. The representative concentration pathways: an overview. *Climatic Change* **2011**, *109*, 5.
(60) Pozzer, A.; Jöckel, P.; Tost, H.; Sander, R.; Ganzeveld, L.; Kerkweg, A.; Lelieveld, J. Simulating organic species with the global atmospheric chemistry general circulation model ECHAM5/MESSy1: a comparison of model results with observations. *Atmos. Chem. Phys.* **2007**, *7*, 2527−2550.
(61) Helmig, D.; Petrenko, V.; Martinerie, P.; Witrant, E.; Rockmann, T.; Zuiderweg, A.; Holzinger, R.; Hueber, J.; Thompson, C.; White, J. W. C.; Sturges, W.; Baker, A.; Blunier, T.; Etheridge, D.; Rubino, M.; Tans, P. Reconstruction of Northern Hemisphere 1950-2010 atmospheric non-methane hydrocarbons. *Atmos. Chem. Phys.* **2014**, *14*, 1463−1483.
(62) Tzompa-Sosa, Z. A.; Mahieu, E.; Franco, B.; Keller, C. A.; Turner, A. J.; Helmig, D.; Fried, A.; Richter, D.; Weibring, P.; Walega, J.; Yacovitch, T. I.; Herndon, S. C.; Blake, D. R.; Hase, F.; Hannigan, J. W.; Conway, S.; Strong, K.; Schneider, M.; Fischer, E. V. Revisiting global fossil fuel and biofuel emissions of ethane. *J. Geophys. Res.: Atmos.* **2017**, *122*, 2493−2512.
(63) Dalsoren, S. B.; Myhre, G.; Hodnebrog, O.; Myhre, C. L.; Stohl, A.; Pisso, I.; Schwietzke, S.; Hoglund-Isaksson, L.; Helmig, D.; Reimann, S.; Sauvage, S.; Schmidbauer, N.; Read, K. A.; Carpenter, L. J.; Lewis, A. C.; Punjabi, S.; Wallasch, M. Discrepancy between simulated and observed ethane and propane levels explained by underestimated fossil emissions. *Nat. Geosci.* **2018**, *11*, 178−186.
(64) Helmig, D.; Thompson, C. R.; Evans, J.; Boylan, P.; Hueber, J.; Park, J. H. Highly elevated atmospheric levels of volatile organic compounds in the Uintah Basin, Utah. *Environ. Sci. Technol.* **2014**, *48*, 4707−4715.
(65) Carter, W. P. L. Development of ozone reactivity scales for volatile organic compounds. *J. Air Waste Manage. Assoc.* **1994**, *44*, 881−899.
(66) Kerkweg, A.; Sander, R.; Tost, H.; Jöckel, P. Technical note: Implementation of prescribed (OFFLEM), calculated (ONLEM), and pseudo-emissions (TNUDGE) of chemical species in the Modular Earth Submodel System (MESSy). *Atmos. Chem. Phys.* **2006**, *6*, 3603−3609.
(67) Fiore, A. M.; Jacob, D. J.; Bey, I.; Yantosca, R. M.; Field, B. D.; Fusco, A. C.; Wilkinson, J. G. Background ozone over the United States in summer: Origin, trend, and contribution to pollution episodes. *J. Geophys. Res.: Atmos.* **2002**, *107* (D15), 4275−4300.
(68) Lindaas, J.; Farmer, D. K.; Pollack, I. B.; Abeleira, A.; Flocke, F.; Fischer, E. V. Acyl peroxy nitrates link oil and natural gas emissions to high ozone abundances in the Colorado Front Range during summer 2015. *J. Geophys. Res.* **2019**, *124*, 2336−2350.
(69) Bogacki, M.; Macuda, J. The influence of shale rock fracturing equipment operation on atmospheric air quality. *Arch. Min. Sci.* **2014**, *59*, 897−912.
(70) Goodman, P. S.; Galatioto, F.; Thorpe, N.; Namdeo, A. K.; Davies, R. J.; Bird, R. N. Investigating the traffic-related environmental impacts of hydraulic-fracturing (fracking) operations. *Environ. Int.* **2016**, *89-90*, 248−260.
(71) Jockel, P.; Tost, H.; Pozzer, A.; Kunze, M.; Kirner, O.; Brenninkmeijer, C. A. M.; Brinkop, S.; Cai, D. S.; Dyroff, C.; Eckstein, J.; Frank, F.; Garny, H.; Gottschaldt, K. D.; Graf, P.; Grewe, V.; Kerkweg, A.; Kern, B.; Matthes, S.; Mertens, M.; Meul, S.; Neumaier, M.; Nutzel, M.; Oberlander-Hayn, S.; Ruhnke, R.; Runde, T.; Sander, R.; Scharffe, D.; Zahn, A. Earth System Chemistry integrated Modelling (ESCiMo) with the Modular Earth Submodel System (MESSy) version 2.51. *Geosci. Model Dev.* **2016**, *9*, 1153−1200.
(72) Parrish, D. D.; Lamarque, J. F.; Naik, V.; Horowitz, L.; Shindell, D. T.; Staehelin, J.; Derwent, R.; Cooper, O. R.; Tanimoto, H.; Volz-Thomas, A.; Gilge, S.; Scheel, H. E.; Steinbacher, M.; Frohlich, M. Long-term changes in lower tropospheric baseline ozone concentrations: Comparing chemistry-climate models and observations at northern midlatitudes. *J. Geophys. Res.: Atmos.* **2014**, *119*, 5719−5736.
(73) Young, P. J.; Naik, V.; Fiore, A. M.; Gaudel, A.; Guo, J.; Lin, M. Y.; Neu, J. L.; Parrish, D. D.; Rieder, H. E.; Schnell, J. L.; Tilmes, S.; Wild, O.; Zhang, L.; Ziemke, J.; Brandt, J.; Delcloo, A.; Doherty, R. M.; Geels, C.; Hegglin, M. I.; Hu, L.; Im, U.; Kumar, R.; Luhar, A.; Murray, L.; Plummer, D.; Rodriguez, J.; Saiz-Lopez, A.; Schultz, M. G.; Woodhouse, M. T.; Zeng, G. Tropospheric Ozone Assessment Report: Assessment of global-scale model performance for global and regional ozone distributions, variability, and trends. *Elementa* **2018**, *6*, 10.
(74) Thoning, K. W.; Tans, P. P.; Komhyr, W. D. Atmospheric carbon-dioxide at Mauna Loa observatory. 2. analysis of the NOAA GMCC data, 1974-1985. *J. Geophys. Res.: Atmos.* **1989**, *94*, 8549−8565.
(75) Cooper, O. R.; Gao, R.-S.; Tarasick, D.; Leblanc, T.; Sweeney, C. Long-term ozone trends at rural ozone monitoring sites across the United States, 1990−2010. *J. Geophys. Res.: Atmos.* **2012**, *117*, 1−24.
(76) Cooper, O. R.; Parrish, D. D.; Ziemke, J.; Balashov, N. V.; Cupeiro, M.; Galbally, I. E.; Gilge, S.; Horowitz, L.; Jensen, N. R.; Lamarque, J. F.; Naik, V.; Oltmans, S. J.; Schwab, J.; Shindell, D. T.; Thompson, A. M.; Thouret, V.; Wang, Y.; Zbinden, R. M. Global distribution and trends of tropospheric ozone: An observation-based review. *Elementa Sci. Anthropocene* **2014**, *2*, 000029.
(77) Chang, K. L.; Petropavlovskikh, I.; Cooper, O. R.; Schultz, M. G.; Wang, T. Regional trend analysis of surface ozone observations from monitoring networks in eastern North America, Europe and East Asia. *Elementa Sci. Anthropocene* **2017**, *5*, 50.
(78) NOAA. NOAA National Centers for Environmental information, Climate at a Glance: National Time Series, http://www.ncdc.noaa.gov/cag/2018. Accessed May 17, 2018.
(79) Rasmussen, D. J.; Fiore, A. M.; Naik, V.; Horowitz, L. W.; McGinnis, S. J.; Schultz, M. G. Surface ozone-temperature relationships in the eastern US: A monthly climatology for evaluating chemistry-climate models. *Atmos. Environ.* **2012**, *47*, 142−153.
(80) Bloomer, B. J.; Stehr, J. W.; Piety, C. A.; Salawitch, R. J.; Dickerson, R. R. Observed relationships of ozone air pollution with temperature and emissions. *Geophys. Res. Lett.* **2009**, *36*, 1−5.
(81) Tzompa, Z.; Henderson, B.; Keller, C.; Travis, K.; Mahieu, E.; Franco, B.; Estes, M.; Helmig, D.; Fried, A.; Richter, D.; Weibring, P.; Walega, J.; Blake, D.; Hannigan, J.; Ortega, I.; Conway, S.; Strong, K.; Turner, A.; Yacovitch, T.; Herndon, S.; Hase, F.; Schneider, M.; Fischer, E. In *The Journey of C2-C5 Alkane Emissions from the Oil and Gas Sector: Atmospheric and Air Quality Implications*, 2018 joint 14th iCACCP Quadrennial Sumposium and 15th IGAC Science Conference, Takamatsu, Kagawa, Japan; September 25-29, 2018.
(82) CFR. Electronic Code of Federal Regulations. https://www.ecfr.gov/cgi-bin/text-idx?tpl=/ecfrbrowse/Title40/40cfr50_main_02.tpl. Accessed Apr 20, 2020.
(83) EPA. EPA, Air Data - Ozone Exceedances, https://www.epa.gov/outdoor-air-quality-data/air-data-ozone-exceedances. Accessed Nov 2019.
(84) EPA. News Releases from Region 08. EPA Reclassifies Denver Area to "Serious" Non-Attainment for Ozone, https://www.epa.gov/newsreleases/epa-reclassifies-denver-area-serious-nonattainment-ozone. Accessed Dec 2019.
(85) Hecobian, A.; Clements, A. L.; Shonkwiler, K. B.; Zhou, Y.; MacDonald, L. P.; Hilliard, N.; Wells, B. L.; Bibeau, B.; Ham, J. M.; Pierce, J. R.; Collett, J. L. Air toxics and other volatile organic compound emissions from unconventional oil and gas development. *Environ. Sci. Technol. Lett.* **2019**, *6*, 720−726.
(86) Chang, C.-Y.; Faust, E.; Hou, X.; Lee, P.; Kim, H. C.; Hedquist, B. C.; Liao, K.-J. Investigating ambient ozone formation regimes in neighboring cities of shale plays in the Northeast United States using photochemical modeling and satellite retrievals. *Atmos. Environ.* **2016**, *142*, 152−170.
(87) McDuffie, E. E.; Edwards, P. M.; Gilman, J. B.; Lerner, B. M.; Dubé, W. P.; Trainer, M.; Wolfe, D. E.; Angevine, W. M.; deGouw, J.;

Williams, E. J.; Tevlin, A. G.; Murphy, J. G.; Fischer, E. V.; McKeen, S.; Ryerson, T. B.; Peischl, J.; Holloway, J. S.; Aikin, K.; Langford, A. O.; Senff, C. J.; Alvarez, R. J.; Hall, S. R.; Ullmann, K.; Lantz, K. O.; Brown, S. S. Influence of oil and gas emissions on summertime ozone in the Colorado Northern Front Range. *J. Geophys. Res.* **2016**, *121*, 8712−8729.

(88) Helmig, D. Air quality impacts from oil and gas development in Colorado. *Elementa Sci. Anthropocene* **2020**, *8*, 4.

https://dx.doi.org/10.1021/acs.est.9b06983
Environ. Sci. Technol. 2020, 54, 12423−12433